Water dynamics in small reverse micelles in two solvents: Two-dimensional infrared vibrational echoes with two-dimensional background subtraction

Emily E. Fenn, Daryl B. Wong, and M. D. Fayer[a)]
Department of Chemistry, Stanford University, Stanford, California 94305, USA

(Received 14 October 2010; accepted 6 December 2010; published online 7 February 2011)

Water dynamics as reflected by the spectral diffusion of the water hydroxyl stretch were measured in $w_0 = 2$ (1.7 nm diameter) Aerosol-OT (AOT)/water reverse micelles in carbon tetrachloride and in isooctane solvents using ultrafast 2D IR vibrational echo spectroscopy. Orientational relaxation and population relaxation are observed for $w_0 = 2$, 4, and 7.5 in both solvents using IR pump–probe measurements. It is found that the pump–probe observables are sensitive to w_0, but not to the solvent. However, initial analysis of the vibrational echo data from the water nanopool in the reverse micelles in the isooctane solvent seems to yield different dynamics than the CCl_4 system in spite of the fact that the spectra, vibrational lifetimes, and orientational relaxation are the same in the two systems. It is found that there are beat patterns in the interferograms with isooctane as the solvent. The beats are observed from a signal generated by the AOT/isooctane system even when there is no water in the system. A beat subtraction data processing procedure does a reasonable job of removing the distortions in the isooctane data, showing that the reverse micelle dynamics are the same within experimental error regardless of whether isooctane or carbon tetrachloride is used as the organic phase. Two time scales are observed in the vibrational echo data, ~1 and ~10 ps. The slower component contains a significant amount of the total inhomogeneous broadening. Physical arguments indicate that there is a much slower component of spectral diffusion that is too slow to observe within the experimental window, which is limited by the OD stretch vibrational lifetime.
 [doi:10.1063/1.3532542]

I. INTRODUCTION

Chemical, biological, geological, and industrial systems often involve water molecules in nanoconfined environments mediating processes at interfaces. The chemical composition of the interface can vary (neutral, charged, hydrophobic, etc.), as well as the size of the confining space. The environment can be a protein pocket or surface, the surface of a cell membrane, the lattice structure of a zeolite, or the water channel in a polyelectrolyte fuel cell membrane. In its bulk form, water exists in an extended hydrogen bond network where water molecules readily make and break hydrogen bonds. Hydrogen bond reformation is a concerted process involving water motions of both the first and second solvation shells.[1,2] Interfaces and nanoscopic confinement can disrupt the rearrangement pathways and slow down hydrogen bond dynamics.[3–5] Important questions involve how an interface influences water dynamics as a function of the size of the system. Observables that report on these influences include the orientational relaxation,[6] vibrational lifetime,[7] and spectral diffusion of the water hydroxyl stretch.[8]

To study confined water, it is useful to employ a system in which the size of the water nanopool can be controlled. The ternary system of the surfactant Aerosol-OT (AOT), water, and a nonpolar phase is often used for this purpose, as reverse micelles of varying water pool diameters, ranging from 1 nm to tens of nanometers, can be made by changing the relative amounts of the components of the mixture.[9–11] The parameter $w_0 = [H_2O]/[AOT]$ determines the water pool size.[11] AOT (Fig. 1) is a charged surfactant molecule with an anionic sulfonate head group and a sodium counter ion. The head group region comes into direct contact with the water pool. The branched, alkyl tails of AOT are immersed in a nonpolar solvent. In large reverse micelles, most of the water resides in a bulklike core while a smaller fraction is influenced by the interface.[12] In small reverse micelles, the interface can perturb the entire water nanopool so that all water molecules deviate from bulklike behavior.[5,12] In addition to having a range of sizes, AOT reverse micelles are spherical, monodispersed, and well characterized, making them a useful system for study. Furthermore, a variety of solvents, including isooctane, hexane, toluene, and carbon tetrachloride, may be used as the nonpolar phase without significantly changing the size or characteristics of the enclosed water pool.[13,14] In this paper, we will address whether changing the identity of the nonpolar phase affects the dynamics of the water pool, even though the static properties, such as size, remain the same.

Techniques which have been employed to study the dynamics of water in AOT reverse micelles include ultrafast infrared (IR) spectroscopy,[3–5,12,15–22] nuclear magnetic resonance,[23,24] fluorescence,[25–30] neutron scattering,[31] dielectric relaxation,[32] and molecular dynamics (MD) simulations.[33–35] These studies collectively agree that water hydrogen bond rearrangement slows down as the reverse micelle size decreases. In particular, ultrafast IR spectroscopy is a potent technique, as it can probe water dynamics on the

a)Electronic mail: fayer@stanford.edu.

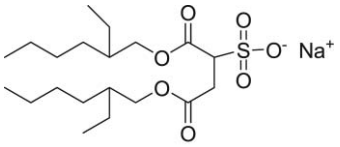

AOT

FIG. 1. Molecular structure of AOT.

relevant picosecond time scale by monitoring observables associated with the water hydroxyl stretching mode.

Spectral diffusion and orientational relaxation in bulk water using dilute HOD in either H_2O or D_2O have been studied with experiments[36–45] and MD simulations.[46–55] HOD is studied rather than pure H_2O or D_2O to eliminate vibrational excitation transfer[56,57] and to simplify the hydroxyl stretch spectrum. For HOD in bulk H_2O, 2D IR vibrational echo experiments show a homogeneous component and spectral diffusion.[38,41] The spectral diffusion occurs on multiple time scales. There is a very fast time scale (<0.4 ps) that MD simulations show arises from very local hydrogen bond fluctuations, mainly of the lengths of the hydrogen bonds.[51,53] The longest time scale for spectral diffusion (1.7 ps) is associated with complete randomization of the hydrogen bond network structure. Pump–probe orientational anisotropy measurements yield a 2.6 ps orientational relaxation time[58] (second Legendre polynomial orientational correlation function decay[6]) following an ultrafast inertial component.[59] The 2.6 ps time arises from jump orientational relaxation.[1,2] The jump reorientation mechanism for orientational relaxation is closely related to the hydrogen bond network randomization that gives rise to the slowest component of the spectral diffusion and the two times, 2.6 ps and 1.7 ps, respectively, are very similar.

In this paper we employ polarization selective IR pump–probe experiments and ultrafast 2D IR vibrational echo experiments. The IR pump–probe experiments measure the vibrational population relaxation and orientational relaxation for three small sizes of micelles, $w_0 = 2$, 4, and 7.5. Each w_0 was prepared in isooctane and in carbon tetrachloride. We also present a study of the spectral diffusion of water in the $w_0 = 2$ reverse micelle using ultrafast 2D IR vibrational echo experiments to monitor the structural evolution of the water hydrogen bond network, also in the two different solvents. $w_0 = 2$ reverse micelles have a water pool diameter of 1.7 nm and contain ~40 water molecules.[12] In $w_0 = 2$, all of the water molecules are strongly influenced by the presence of the interface, but not all hydroxyl groups are necessarily hydrogen bonded to a sulfonate.

Isooctane has been widely used as the nonpolar phase for AOT reverse micelle systems in a variety of experiments ranging from viscosity and density characterizations to x-ray scattering and ultrafast IR measurements.[10,12,60,61] MD simulations have also utilized isooctane as the nonpolar phase. It is therefore important to know whether experiments carried out in different solvents may be compared. In this paper we compare results for the solvents isooctane and CCl_4. We find within experimental error that the spectra, population relaxation, and orientational relaxation remain constant for a given w_0 regardless of the solvent. Initially the spectral diffusion of the OD stretch of dilute HOD in H_2O in $w_0 = 2$ reverse micelles appears to be much faster when the solvent is isooctane than when it is CCl_4. However, the interferograms that are Fourier transformed to obtain the 2D IR vibrational echo spectra are distorted in the isooctane solvent system. In the absence of HOD and in the absence of any water, two situations in which no signal should be produced, the AOT/isooctane sample gives a signal in the vibrational echo experiment but the AOT/CCl_4 sample does not. Isooctane by itself gives no signal. A method was developed in which the interferogram signals from the AOT/isooctane/H_2O sample were recorded and subtracted from the interferogram signals obtained from the AOT/isooctane/HOD/H_2O sample. When this 2D background is removed, the spectral diffusion from the samples with CCl_4 and isooctane become similar. Because of the distortions introduced by the isooctane solvent, CCl_4 is a better solvent for the 2D IR experiments. These results show that the experimental results may be directly compared even if different solvents are used as the nonpolar phase.

II. EXPERIMENTAL PROCEDURES

Isooctane, carbon tetrachloride, H_2O, and D_2O (Sigma-Aldrich) were used as received. Aerosol-OT (sodium bis(2-ethylhexyl) sulfosuccinate, AOT) was vacuum dried for at least 1 week before sample preparation. 0.5 M stock solutions of AOT were prepared in isooctane and in carbon tetrachloride. The residual water content was determined by Karl Fischer titration to be $w_0 = 0.14$ in the isooctane stock solution and $w_0 = 0.2$ in the carbon tetrachloride stock solution. Reverse micelle samples were prepared by mass by adding appropriate amounts of a stock solution of 5% HOD in H_2O to measured quantities of the AOT stock solutions to make the desired w_0.

The OD stretch of dilute HOD in H_2O is studied because it prevents vibrational excitation transfer processes from causing artificial decays of the orientational correlation function and the frequency–frequency correlation function (FFCF) (spectral diffusion).[56,57] MD simulations have shown that a small percentage of HOD does not change the structure and properties of H_2O and that experiments on the OD stretch yield the dynamics of water.[52] The samples for IR absorption and ultrafast experiments were contained in sample cells consisting of two calcium fluoride windows separated with a Teflon spacer. The Teflon spacer thickness was chosen such that the optical density in the OD stretch region was ~0.1 for 2D IR echo experiments and ~0.5 for pump–probe experiments.

In the laser system, a Ti:sapphire oscillator seeds a regenerative amplifier, the output of which pumps an optical parametric amplifier (OPA). The output of the OPA is difference frequency mixed in a $AgGaS_2$ crystal to generate ~70 fs pulses at ~4 μm (2500 cm^{-1}). The wavelength of the IR light is tuned to the frequency of the peak absorption of the OD stretch spectrum, which is 2565 cm^{-1} for $w_0 = 2$. In the 2D IR experiments, the IR beam is split into three excitation pulses and a fourth beam, the local oscillator (LO). The three excitation pulses are time ordered, with pulses 1 and 2 traveling

along variable delay stages. The first pulse creates a coherence consisting of a superposition of the $v = 0$ and $v = 1$ vibrational levels. During the evolution period τ, the phase relationships between the oscillators decay. The second pulse reaches the sample at time τ and creates a population state in either $v = 0$ or $v = 1$. A time T_w (the waiting period) elapses before the third pulse arrives at the sample to create another coherence that partially restores the phase relationships. Rephasing of the oscillators causes the vibrational echo signal to be emitted at a time $t \leq \tau$ after the third pulse. During T_w, spectral diffusion occurs as the water molecules sample different environments due to dynamic structural evolution of the system. The frequencies of the OD vibrational oscillators evolve (spectral diffusion) as the water network structure changes. The vibrational echo signal is spatially and temporally overlapped with the LO for heterodyned detection. The heterodyned signal is frequency dispersed by a monochromator and detected on a 32 element mercury cadmium telluride detector. At a fixed T_w, τ is scanned to generate a 2D IR vibrational echo spectrum. Then T_w is changed and another 2D spectrum is recorded. The time evolution of the 2D spectra provides the information on spectral diffusion.

The correlation spectra are vulnerable to errors in delay stage timing as well as linear chirp. The chirp in the IR pulses is measured by a frequency resolved optical gating technique[62] in a nonresonant version of the experimental sample (no OD chromophore). The chirp is corrected by changing the amount of calcium fluoride through which the IR beam travels. The temporal overlaps between pulses 1, 2, and 3 are set through a three pulse cross-correlation experiment in the nonresonant sample. An automatic computer controlled program periodically resets the timing between pulses 1, 2, and 3 to prevent temporal overlap drifts that are significant to the experiment. In this process, data collection on the experimental sample is halted and a computer controlled pneumatic translation stage moves the nonresonant sample into the experimental position. The intensity level signal is then directed into a single element IR detector using a computer controlled mirror. The temporal overlap of the three stages is checked and corrected, if necessary, after which the experimental sample is moved back into position.

The timing between the signal and LO is also checked periodically. Before the experiment, with pulses 1, 2, and 3 having zero delays, the signal from the resonant experimental sample is combined with the local oscillator and directed into a single element detector. The LO is scanned to record a temporal interferogram which is used as a reference during the experiment. After the zero of time of pulses 1, 2, and 3 is reset and the resonant experimental sample is back in place, the signal combined with the local oscillator is again directed into the single element detector using a computer controlled mirror. The local oscillator is scanned, and the temporal interferogram is compared to the one recorded at the beginning of the experiment. The local oscillator delay stage position is then reset to match the measured interferogram to the initially recorded interferogram. Because there are a very large number of oscillations, the timing can be set accurately. The periodic retiming of pulses 1, 2, and 3 and the LO relative to the signal eliminates the drift which can be detrimental to data collection. The signal to noise of the data is improved by averaging the interferograms from many scans. The procedure outlined above enables data to be collected for days without timing errors distorting the data. When a new sample is used, the initial measurements must be repeated to account for the differences in the properties of the samples.

Center line slope (CLS) analysis[63–65] of the 2D IR vibrational echo spectra is used to analyze the data. In the CLS technique, slices are cut through the 2D spectra parallel to the ω_m (detection) axis and fit to Gaussian line shapes to obtain the peak positions for each slice. The peak positions are plotted versus ω_τ (the excitation axis frequency intercepted by each slice) over a range of frequencies about the center of the spectrum and fit with a linear regression to find the slope of the line. These slopes are obtained for each T_w and plotted versus T_w. The CLS method of data analysis is a useful method for extracting information from the 2D data. It is independent of a specific model of the spectral diffusion dynamics. A fit to the CLS data using, for example, a multiexponential model yields time constants that can be compared for different systems. MD simulations can be used to calculate the 2D IR vibrational echo spectra, and then the CLS can be obtained from the simulated 2D spectra and compared to data.

It has been shown theoretically that the CLS can be used to determine the FFCF under the assumption of Gaussian fluctuations.[63,65] The FFCF is a key to understanding the structural evolution of molecular systems in terms of amplitudes and time scales of the dynamics. The FFCF is the joint probability distribution that the frequency has a certain initial value at $t = 0$ and another value at a later time t. The FFCF connects the experimental observables to the underlying dynamics. Once the FFCF is known, all linear and nonlinear optical experimental observables can be calculated by time-dependent diagrammatic perturbation theory.[66] However in bulk water, non-Condon effects and deviation from Gaussian fluctuations play a role in the nature of the 2D IR vibrational echo spectra and other observables.[67,68] Non-Condon effects account for a varying transition dipole with absorption frequency.[67,68] The FFCF is based on a theoretical methodology that does not include non-Condon effects. Simulations of bulk water using the Gaussian approximation or simulations without the Gaussian approximation, which include non-Condon effects, and other details show that variations in the simulations of the experimental observables using different water models are as large as differences that arise from making or not making the Gaussian approximation.[38,41,53,68] For water nanopools in reverse micelles, which are even more complex than bulk water, the difficulties of trying to extract useful information from 2D IR spectra using full simulations are monumental. Therefore, employing the CLS to determine the FFCF, in spite of its approximate character, is a very useful approach for determining the time scales of structural fluctuation and for comparing one system to another.

The FFCF can be described with the form

$$C_1(t) = \langle \delta\omega_{1,0}(\tau_1)\delta\omega_{1,0}(0)\rangle = \sum_i \Delta_i^2 \exp\left(\frac{-t}{\tau_i}\right). \quad (1)$$

The Δ_i are the frequency fluctuation amplitudes of each component and the τ_i are their associated time constants. If $\Delta\tau < 1$ for one component of the FFCF, then Δ and τ cannot be determined separately, but rather give rise to a motionally narrowed homogeneous contribution to the absorption spectrum with pure dephasing width given by $\Gamma_p = \Delta^2\tau = 1/\pi T_2^*$, where T_2^* is the pure dephasing time and Γ_p is the pure dephasing linewidth. The total homogeneous dephasing time, T_2, also has contributions from the vibrational lifetime and orientational relaxation. T_2 is given by

$$\frac{1}{T_2} = \frac{1}{T_2^*} + \frac{1}{2T_1} + \frac{1}{3T_{or}}, \tag{2}$$

where T_2^*, T_1, and T_{or} are the pure dephasing time, vibrational lifetime, and orientational relaxation time, respectively. The total homogeneous linewidth is $\Gamma_h = 1/\pi T_2$. The homogeneous linewidth is dominated by pure dephasing. The CLS decay yields the normalized FFCF. Detailed procedures for converting the CLS measurement into the FFCF have been described previously.[65] By combining the CLS with the linear absorption spectrum, the full FFCF is obtained including the homogeneous component.

In the polarization and wavelength selective pump–probe experiments, the IR beam is split into two pulses, a weak probe and an intense pump. The pump is polarized at 45° relative to the horizontally polarized probe pulse. The pump and probe impinge on the sample, after which the polarization of the probe is resolved parallel and perpendicular (+/–45°, respectively) to the pump using a polarizer on a computer controlled rotation stage. The polarization is again set to horizontal before entering the monochromator in order to eliminate problems from polarization-dependent diffraction and reflection efficiencies of the monochromator. Again, the frequency-dispersed signal is detected by a 32 element mercury cadmium telluride detector. The measured parallel and perpendicular signals contain information about the population relaxation and orientational dynamics of the water molecules (HOD),

$$I_{\parallel} = P(t)(1 + 0.8C_2(t)), \tag{3}$$

$$I_{\perp} = P(t)(1 - 0.4C_2(t)), \tag{4}$$

where $P(t)$ is the vibrational population relaxation and $C_2(t)$ is the second Legendre polynomial orientation correlation function for a dipole transition. The parallel and perpendicular signals are combined to give the pure population relaxation,

$$P(t) = I_{\parallel} + 2I_{\perp}. \tag{5}$$

The signals may also be combined to give the anisotropy $r(t)$, from which $C_2(t)$ can be extracted,

$$r(t) = \frac{I_{\parallel} - I_{\perp}}{I_{\parallel} + 2I_{\perp}} = 0.4C_2(t). \tag{6}$$

III. RESULTS AND DISCUSSION

A. Infrared absorption spectroscopy and pump-probe experiments

Figure 2 shows the linear absorption spectra of the OD stretch in H_2O in three small reverse micelles in carbon tetrachloride and isooctane solvents, in addition to the spectrum of bulk water for comparison. The spectra for a given w_0 for the two solvents are identical within experimental error, which supports previous experimental results that concluded that the micelle size varies little with the identity of the nonpolar solvent.[13] As has been discussed extensively previously,[12] the spectra exhibit a systematic blue shift as the size of the micelle decreases. Compared to the peak absorption of the OD stretch of HOD in bulk water that falls at 2509 cm^{-1}, the OD spectrum of water in the $w_0 = 2$ micelle has its peak absorption at 2565 cm^{-1}. When OD is bound to sulfonate moieties, the stretching spectrum is blue shifted relative to OD bound to a water oxygen. The spectra with higher proportions of interfacial waters have greater blue shifts.[3,5,12]

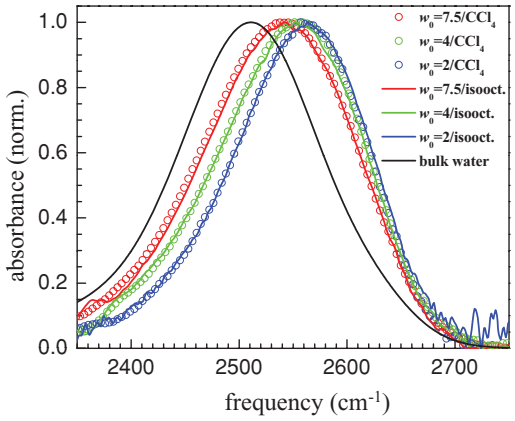

FIG. 2. FT-IR absorption spectra for bulk water and water inside AOT/isooctane and AOT/CCl_4 reverse micelles. The spectra of reverse micelles of the same size in different solvents are identical. As the micelle size decreases, the spectra systematically shift to the blue.

Moilanen *et al.* recently studied the orientational dynamics of water molecules at the interface in AOT reverse micelles in isooctane, showing that in large reverse micelles, the dynamics of water molecules at the interface and in the core (bulklike water in the center of large water nanopools) may be separated.[3,5] Each region has dynamics with its own characteristic decay constants. The water dynamics for small reverse micelles ($w_0 \leq 5$) exhibit reorientation dynamics that are no longer separable into core and shell values.[5] The orientational relaxation of the OD stretch of HOD in H_2O in $w_0 = 2$ reverse micelles has an ultrafast inertial component (<200 fs), a fast component (~1 ps), which has been attributed to wobbling-in-a-cone,[5,19,69] and a very slow component of 110 ± 40 ps.[5] Because of limitations in the longest time that can be measured caused by the vibrational lifetime, even slower relaxation may occur.

Besides orientational relaxation, population relaxation (vibrational lifetime) behavior also provides insight into the structure and environment of water molecules in heterogeneous environments such as reverse micelles. When an oscillator becomes excited, its vibrational energy will dissipate into a combination of low frequency modes, such as bending modes, torsions, and bath modes, which sum to the original energy.[7,70] In unrestricted environments such as bulk water, vibrational energy readily dissipates via these modes.

TABLE I. Wavelength-dependent vibrational relaxation times for AOT reverse micelles in CCl_4 and isooctane.

Sample	Parameter	2590 cm^{-1}	2610 cm^{-1}	2620 cm^{-1}	2640 cm^{-1}
$w_0 = 2/CCl_4$	A_1	0.13	0.08	1.0	1.0
	τ_{vib1} (ps)	2.0	2.0	7.4	8.1
	τ_{vib2} (ps)	7.3	7.5	...	...
$w_0 = 2$/isooctane	A_1	0.10	0.05	1.0	1.0
	τ_{vib1} (ps)	1.9	1.9	7.2	7.9
	τ_{vib2} (ps)	6.7	7.1	...	...
$w_0 = 4/CCl_4$	A_1	0.22	0.15	0.13	0.10
	τ_{vib1} (ps)	2.0	2.0	2.0	2.0
	τ_{vib2} (ps)	6.4	6.6	6.9	7.4
$w_0 = 4$/isooctane	A_1	0.27	0.19	0.14	0.17
	τ_{vib1} (ps)	2.0	2.0	2.0	2.0
	τ_{vib2} (ps)	6.2	6.4	6.5	6.7

Error bars are ±0.2 ps for the time constants, τ_{vib}, and ±0.4 for the amplitudes, A_1.

When a solute or interface disrupts the hydrogen bonding network, pathways that were available in the bulk may no longer be accessible by the water molecules. Consequently, vibrational lifetimes are very sensitive to local environments. For instance, the two vibrational lifetimes observed in large AOT reverse micelles reflect a population of water molecules hydrogen bonded to other water molecules and a second population of water molecules hydrogen bonded to the sulfonate head groups. The lifetimes associated with these populations are 1.8 and 4.3 ps, respectively.[3] Previous experiments reported single exponential vibrational lifetime behavior in very small AOT reverse micelles ($w_0 = 2$ and 5) at all wavelengths,[12] but upon more rigorous analysis, we find that there is a slight wavelength dependence to the vibrational lifetime. Well to the blue side of the OD stretch vibrational spectrum, starting at ~2620 cm^{-1}, the vibrational lifetime is single exponential, but the single lifetime varies somewhat with wavelength. For instance, at 2620 cm^{-1} the lifetime is 7.4 ps, while at 2640 cm^{-1} it is 8.1 ps. At lower frequencies in the absorption spectrum, the vibrational lifetime displays biexponential behavior. For the $w_0 = 2/CCl_4$ sample, there is a relatively fast lifetime component of 2.0 ps with a small amplitude (13% and 8% at 2590 and 2610 cm^{-1}, respectively) while a second slower component of ~7.5 ps makes up the rest of the amplitude. Again, there is a slight wavelength dependence to the value of this second time constant (see Table I).

The existence of two separate lifetimes does not necessarily mean that there are two distinct ensembles of water molecules as there are in larger reverse micelles. In larger reverse micelles ($w_0 \geq 7.5$), there are distinct core and interfacial regions of water molecules, each with associated vibrational lifetimes. In $w_0 = 2$, the water pool is too small to have a distinct core region. A distinct core exists if there are at least some water molecules with first and second solvation shells that do not directly interact with the interface. In the very small reverse micelles, the majority of water molecules interacts with the interface. However, some of the hydroxyls will be hydrogen bonded to oxygens of other water molecules rather than to sulfonate head groups. Thus there are two types of local environments for the OD stretch vibrational relaxation. As vibrational lifetimes are extremely sensitive to local environment, these two environments give rise to two lifetimes. As the short lifetime, ~2 ps, is very similar to the lifetime found in bulk water, we assign this to ODs bound to water oxygens. This assignment is further supported by the lack of this lifetime component on the blue side of the spectrum which arises from water molecules bound to sulfonates, and these ODs display only the long lifetime. The water molecules are not segregated into two regions with distinct lifetimes as they are in large reverse micelles. In contrast, orientational dynamics rely on concerted motions involving many water molecules.[1,2] Therefore, in very small reverse micelles, orientational relaxation involves a single collective ensemble of water molecules while vibrational relaxation is sensitive to the differences in the immediate environment of a hydroxyl.

The $w_0 = 4/CCl_4$ reverse micelle system also shows two-component vibrational lifetime behavior with one time constant equal to 2.0 ps and the second time constant ranging from 6.4 to 7.4 ps, depending on the wavelength (Table I). Again, local heterogeneities in hydrogen bonding inside the reverse micelle yield separate lifetimes even if the orientation dynamics do not yield separate orientation times. The vibrational lifetimes were measured for both the CCl_4 and isooctane systems (Table I). Within experimental error, the observed lifetimes and associated amplitudes do not vary with solvent, further supporting the idea that the water nanopools remain constant regardless of the nonpolar phase's identity. Figures 3 and 4 display population and orientational relaxation data, respectively, for the three micelles in both solvents at a common wavelength. Within experimental error, the data are invariant with solvent.

Vibrational and orientational relaxation parameters were also measured for the $w_0 = 7.5/CCl_4$ reverse micelle system, listed in Table II. Unlike the two smaller reverse micelle sizes, $w_0 = 7.5$ shows two-component behavior in both vibrational lifetime and orientational relaxation. The functional form and usage of the two-component model have been addressed in depth in previous publications.[3–5,71] The $w_0 = 7.5$ reverse micelles behave the same as the $w_0 = 10$ reverse micelles studied previously.[5] Distinct core and interfacial regions exist for $w_0 = 7.5$, but unlike the larger reverse micelles ($w_0 \geq 16.5$), the core region is not purely bulklike. Instead, its parameters are 2.1 ps for vibrational lifetime and 4.4 ps for orientation,

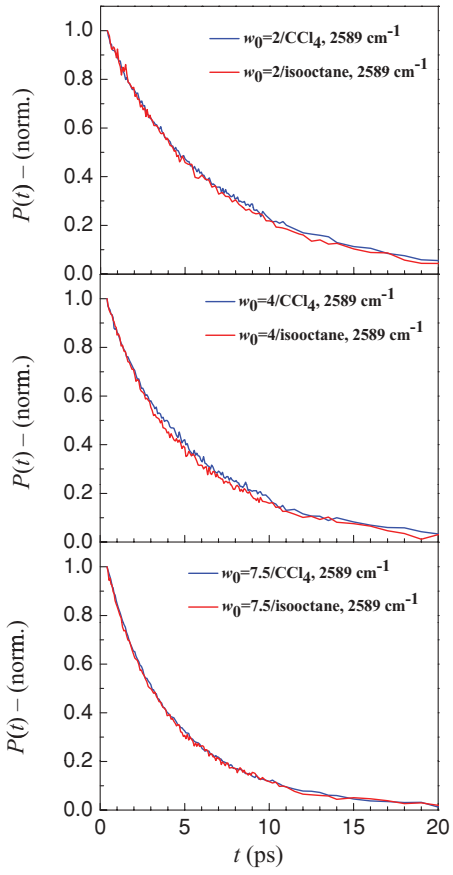

FIG. 3. Population relaxation data for water in the three sizes of small reverse micelles showing the invariance with nonpolar phase.

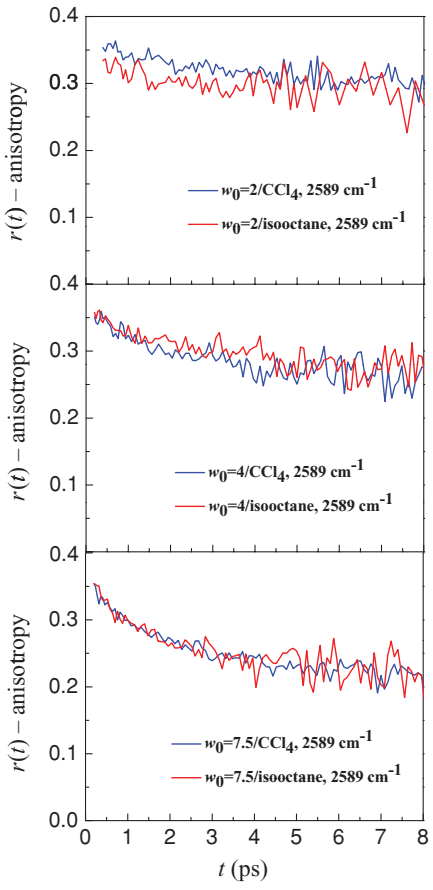

FIG. 4. Orientation relaxation data for water in the three sizes of small reverse micelles, again showing the invariance with the nonpolar phase.

which are slower than the bulk water values of 1.8 ps for vibrational lifetime and 2.6 ps for orientational relaxation. The interfacial values are 5.5 ps for vibrational lifetime and 30 ps for orientational relaxation. The corresponding values are also listed for the reverse micelles in isooctane, and they further show the insensitivity of the dynamics to solvent. Therefore, the spectra, lifetimes, and orientational relaxation times are the same within experimental error whether the solvent is isooctane or CCl_4.

B. 2D IR vibrational echo experiments

Figure 5 displays 2D IR vibrational echo spectra for $w_0 = 2$ in CCl_4 at a series of T_w's. The ω_τ axis is the frequency axis for the first radiation field interaction (first pulse) and the ω_m axis is the frequency of the vibrational echo emission, which corresponds to the frequency of the third radiation field interaction (third pulse). The positive peak along the diagonal is from the 0 to 1 vibrational transition, while the negative-going peak below it arises from vibrational echo emission at the 1–2 transition frequency. The 1–2 peak is shifted along the ω_m axis by the vibrational anharmonicity. The spectrum is very elongated along the diagonal at early T_w, meaning that there is a high probability that an oscillator excited at one frequency will be detected at the same frequency. As time progresses, the elongated peak becomes more symmetric as the oscillators sample different environments, causing changes in frequency (spectral diffusion). At the longest T_w's for $w_0 = 2$, spectral diffusion is not complete. There is still significant elongation along the diagonal.

TABLE II. Two-component model vibrational lifetimes and orientational relaxation parameters for $w_0 = 7.5$ reverse micelles in CCl_4 and isooctane.

w_0	τ_{vib1} (ps)	τ_{vib2} (ps)	τ_{or1} (ps)	τ_{or2} (ps)
7.5/CCl_4	2.1	5.5	4.4	30
7.5/isooctane	2.1	5.6	4.4	21

Error bars are ±0.2 ps for time constants, τ_{vib}, ±0.5 ps for τ_{or1}, and ±5 ps for τ_{or2}.

The 2D IR spectra can be analyzed with the CLS method[63–65] described in the experimental section. The CLS data for $w_0 = 2$ in CCl_4 are shown in Fig. 6(a). The vibrational lifetime prevents the acquisition of data at longer times. For the physical reasons discussed below, we assume that there is a very slow component to the spectral diffusion that is beyond the experimental time window. In fitting the CLS, the very slow component is modeled as being infinitely slow, so the fit involves a sum of exponentials plus a constant (Table III). In addition to the homogeneous component, there is a fast time constant of 0.9 ps, an intermediate time constant of 10 ps, and an offset reflecting the very slow dynamics. Using the CLS data and the linear absorption line shape, the FFCF was determined.[65] The results are presented in Table IV.

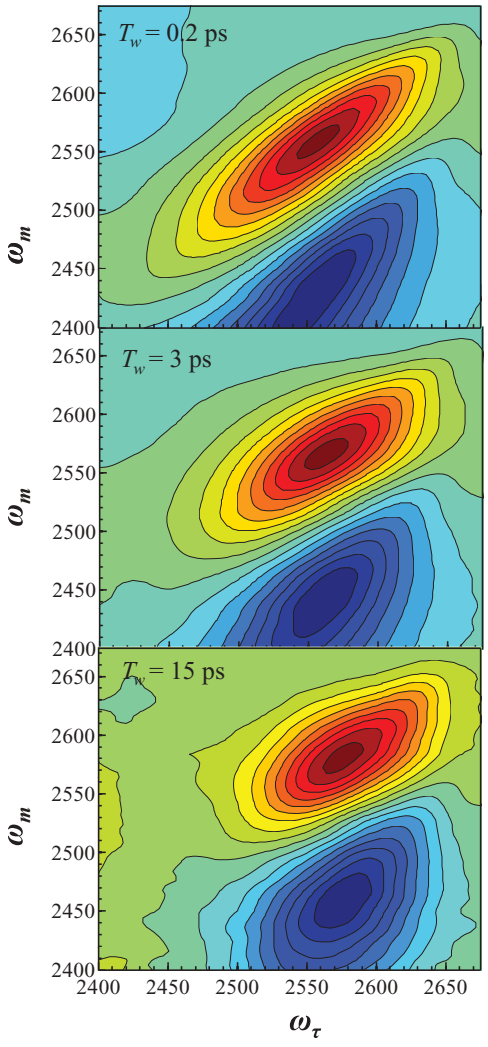

FIG. 5. 2D IR correlation spectra for $w_0 = 2/CCl_4$ at a range of T_w's.

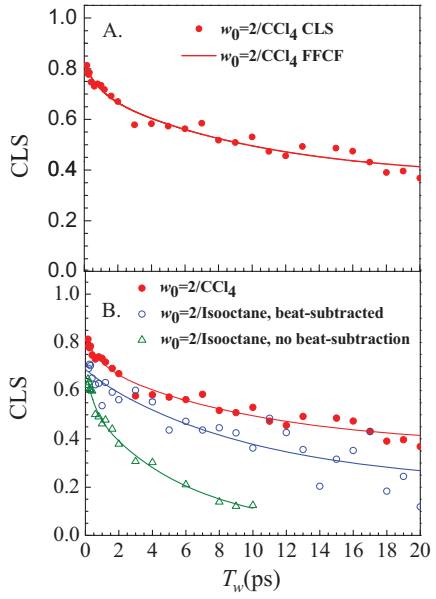

FIG. 6. (a) Experimental CLS data for $w_0 = 2/CCl_4$ reverse micelles. The line through the data is the normalized frequency–frequency correlation function for $w_0 = 2$. (b) Experimental center line slope results: $w_0 = 2/CCl_4$ (solid dots), $w_0 = 2$/isooctane beat subtracted data showing decent agreement with results in CCl_4 (hollow dots), and nonbeat subtracted $w_0 = 2$/isooctane data showing extremely fast decay (triangles). The line through the top curve is the normalized FFCF for that sample, while the bottom two lines are the bi-exponential fits from Table V.

Previously, echo peak shift measurements and diagrammatic perturbation theory were used to obtain the FFCF parameters for $w_0 = 2$ AOT.[12,14,20] However, these experiments only made measurements out to 2 ps. Here, measurements were made to 20 ps, and many more T_w time points were measured.[35]

Our initial echo experiments used isooctane as the organic phase because the AOT/water/isooctane microemulsion system has been well characterized, both in terms of steady-state characteristics and water hydrogen bonding dynamics. In addition, reverse micelles may be made up to very large diameters in isooctane, whereas those in CCl_4 are only stable up to $w_0 \sim 10$.[12,72] The bottom curve in Fig. 6(b) displays the CLS for $w_0 = 2$ with isooctane as the solvent. The top curve is the same data as Fig. 6(a); the solvent is CCl_4. We will return to the middle curve below. In spite of the fact that the spectra, vibrational lifetimes, and orientational relaxation were identical in the two solvents, initially it appeared that the spectral diffusion was very different.

Examination of the raw interferogram data for the isooctane solvent showed strange behavior. Figure 7(a) displays an echo interferogram (raw data) of $w_0 = 2$ AOT/isooctane at 2580 cm^{-1} at $T_w = 1$ ps. There are several peculiar features in this interferogram. First, there is a small beat around –0.3 ps. In addition, the amplitude rises very sharply as zero is approached from negative time with the peak of the intensity at ~0 ps. The rising edge should be determined by the free induction decay, which is the Fourier transform of the absorption spectrum. The observed rising side is too fast. There is little to no peak shift, and the rephasing (positive time) region has a strange, concave shape. The beat pattern and strange shapes were reproducible and found at nearly all detection wavelengths and T_w's, with some exceptions at wavelengths far to the red. Similar patterns were observed for other w_0's in isooctane as well. Figure 7(b) displays an interferogram from an AOT reverse micelle of the same w_0, T_w, and detection wavelength, but the nonpolar phase is CCl_4. This interferogram looks completely normal. There are no beats and the rising edge is slower, in accord with the free induction decay.

TABLE III. CLS data biexponential with an offset fit parameters. A_i — amplitudes; t_i — time constants; y_0 — offset.

A_1	t_1 (ps)	A_2	t_2 (ps)	y_0
0.10	0.9 ± 0.1	0.35	10 ± 1	0.36

Error bars for A_1, A_2, and y_0 are ±0.01.

TABLE IV. Frequency-frequency correlation function parameters. T_2 — homogeneous dephasing time; Δ_i — amplitudes; t_i — time constants.

T_2 (ps)	Δ_1 (cm^{-1})	t_1 (ps)	Δ_2 (cm^{-1})	t_2 (ps)	Δ_3 (cm^{-1})
0.17 ± 0.02	19 ± 2	0.9 ± 0.1	37 ± 1	10 ± 1	37 ± 1

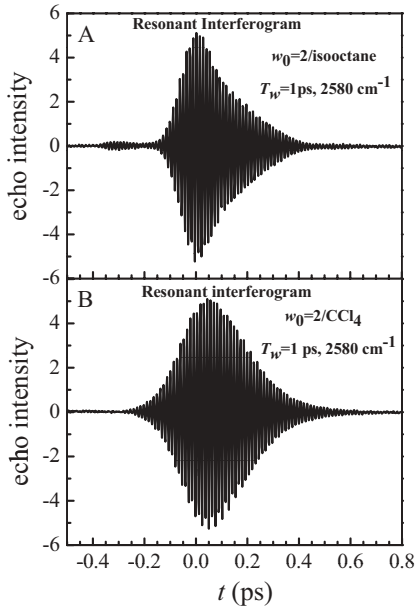

FIG. 7. Interferogram data. (a) Resonant interferogram in AOT/isooctane for $w_0 = 2$ at $T_w = 1$ ps and 2580 cm^{-1}, showing the strange beat behavior. (b) AOT/CCl_4 interferogram for $w_0 = 2$ at $T_w = 1$ ps and 2580 cm^{-1}, showing normal echo behavior.

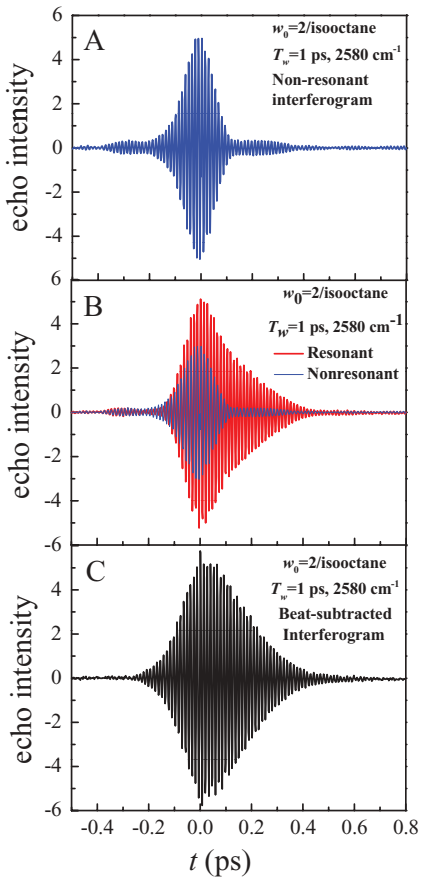

FIG. 8. (a) Interferogram for nonresonant pure H_2O in AOT/isooctane, showing strange beat behavior. (b) The red and blue interferograms respectively show the resonant and nonresonant $w_0 = 2$ interferograms at $T_w = 1$ ps and 2580 cm^{-1} used for beat subtraction. (c) Results of the beat subtraction method in isooctane. The interferogram looks a lot cleaner and similar to the interferogram in Fig. 7(b).

To determine the reason for the unusual nature of the interferograms in the isooctane solvent and the possible influence on the CLS [the bottom curve in Fig. 6(b)], we ran a series of vibrational echo experiments on samples which should have yielded no echo signal. One experiment was to see if pure isooctane generated an echo signal. It did not, and nor did pure carbon tetrachloride. We also ran the AOT/water/isooctane $w_0 = 2$ reverse micelle without any OD probe (just pure water in the micelle core) and obtained the interferogram shown in Fig. 8(a). In addition to the large component centered on $\tau = 0$, the negative time beat seen in Fig. 7(a) is present and a positive beat can also be seen. This second beat was obscured in Fig. 7(a) by the much larger signal produced by the OD stretch. We also obtained interferogram data on a sample of 0.5 M AOT solution in isooctane from which the reverse micelles were made. This sample had virtually no water ($w_0 = 0.14$). The stock solution yielded essentially identical data to the $w_0 = 2$ sample without HOD (Fig. 8(a)), demonstrating that the addition of H_2O does not affect the beat patterns. In addition, we made measurements on the CCl_4 stock solution (0.5 M AOT in CCl_4). This sample gave no signal. We only found the beating interferograms for samples containing both isooctane and AOT.

In a very different context, multicolor stimulated Raman experiments by John Wright studying AOT/D_2O reverse micelles in octane in the same IR spectral range found anomalous components in the 2D spectrum.[73] Following discussions about the experiments presented here, they found that the anomalous band was even larger when they used isooctane as the solvent. We have conducted preliminary experiments with cyclohexane as the solvent and pure H_2O in the reverse micelles. This nonresonant solution does not yield a vibrational echo signal. These results suggest that the interactions between methyl groups of the solvent and the AOT influence the nature of the system and give rise to the type of signal displayed in Figs. 7(a) and 8(a). In contrast to AOT/CCl_4, the FT-IR spectrum of AOT/isooctane displays some small absorptions in the spectral region of the OD absorption. However, none of these in particular could be assigned as being responsible for the beating interferogram shown in Figs. 7(a) and 8(a). Again, it is important to note that neither AOT nor isooctane by themselves gives rise to signals. The supplementary information for this paper includes FT-IR spectra of the solvents and stock solutions and provides additional details concerning the nature of the beats.[76]

In an attempt to remove distortions from the isooctane data, we ran two sets of vibrational echo experiments back-to-back, with one sample being the normal resonant $w_0 = 2$ AOT/isooctane reverse micelle with 5% HOD/H_2O and the other being the $w_0 = 2$ sample with pure H_2O. Running the samples right after one another preserved the laser conditions between the experiments as much as possible to make the data processing more reliable. Using the two sets of data, "beat subtracted" sets of interferograms were obtained. Figure 8(b) shows the pure H_2O interferogram (blue) superimposed on the interferogram taken with HOD (red) for $w_0 = 2$ at 1 ps and 2580 cm^{-1}. Using the region of the negative time beat, the pure H_2O data were multiplied by a constant so that its

TABLE V. Biexponential fit parameters for beat subtracted $w_0 = 2$/isooctane and $w_0 = 2$/isooctane without beat subtraction.

Sample	A_1	t_1 (ps)	A_1	t_2 (ps)	y_0
$w_0 = 2$/isooctane with beat subtraction	0.01	0.9	0.47	10	0.21
$w_0 = 2$/isooctane without beat subtraction	0.16	0.44	0.52	5.7	0.02

amplitude matched the amplitude of the beat from the HOD data. In addition, a small <2 fs adjustment in time was made to match the phases of the two sets of oscillations in the negative time beat region. The pure H_2O interferogram (blue) was then subtracted from the HOD interferogram (red). The result of the subtraction is shown in Fig. 8(c). This interferogram has been scaled for clarity. The interferogram after subtraction is virtually identical to the one shown in Fig. 7(b). The negative time beat is gone. The rising edge has the correct shape as does the positive time decay.

This subtraction procedure was done at every wavelength for every T_w (automated by a MATLAB fitting routine). It is important to state that this procedure is fraught with difficulties. Two completely separate sets of vibrational echo experiments need to be conducted on two samples. Just switching the samples, which of course are in different sample cells, can introduce error. After the subtraction procedure was applied to all of the interferograms from the isooctane sample, 2D IR vibrational echo spectra were constructed in the normal manner. From these spectra the T_w dependent CLS was obtained. The plot of this CLS curve is the middle curve in Fig. 6(b). While the middle curve in Fig. 6(b) (beat subtracted isooctane) is not identical to the top curve (CCl_4), they are very similar. From the CLS plots the frequency–frequency correlation functions were calculated and compared. We found little difference between the isooctane and CCl_4 data. The FFCF for the reverse micelles in CCl_4 is given in Table IV. However, due to the inherent noise generated by so many data processing steps in the beat subtraction, especially at long T_w's, we feel more confident in our ability to fit and interpret the CCl_4 data. Both the CCl_4 and isooctane CLS data sets can be fit with the same time constants shown in Table III, with differences only in the amplitudes. The biexponential fit parameters for the middle and bottom curves in Fig. 6(b) are listed in Table V. Without beat subtraction, the data from the reverse micelles in isooctane decay very quickly [bottom curve, Fig. 6(b)] and bear no resemblance to the CCl_4 data [top curve, Fig. 6(b)]. After beat subtraction, the time constants of the CLS (Table V) are the same as those found for the system with CCl_4 (Table III) as the solvent.

Our main purpose in pursuing the isooctane 2D IR spectrum background subtraction experiments was to show that there is little difference in dynamics with different solvents, allowing us to compare our experimental CCl_4 data with other studies conducted with isooctane as the solvent. The lack of difference in the spectral diffusion between solvents is perhaps not too surprising, as the infrared spectra and pump–probe experiments show perfect agreement in absorption line shapes (Fig. 2), vibrational relaxation (Fig. 3), and reorientation dynamics (Fig. 4) between the two solvents. We conclude that water nanopools in small reverse micelles of the same size prepared in CCl_4 and in isooctane have identical characteristics.

We can now discuss the FFCF parameters given in Table IV. In bulk water, the FFCF is characterized with two time constants of ~400 fs and 1.7 ps and a motionally narrowed homogeneous component.[74] The homogeneous component and the 400 fs component have been attributed to fast, local fluctuations in the hydrogen bonding network, while the 1.7 ps time constant is associated with complete structural randomization through global hydrogen bond rearrangement. As discussed in Sec. I, bulk water orientational relaxation has a time constant of 2.6 ps, which is attributed to jump reorientation.[1,2] The two time constants for spectral diffusions and orientational relaxation are very similar because the mechanisms that give rise to them are very similar. However, in the $w_0 = 2$ reverse micelle water nanopools, there are at least three decay times in addition to a homogeneous component. In analogy to bulk water, the 0.9 ps decay may be the result of local hydrogen bond fluctuations that are slowed compared to bulk water because of the constraints placed on the hydrogen bond network by the interactions with the interface. The offset in the FFCF parameters reflects the dynamics that are so slow that they are outside the experimental time window, which is limited by the vibrational lifetime. Simulations show that there are very slow dynamics that contribute at long time to the FFCF.[35] For example, water molecules that are surrounded by other water molecules will have a different distribution of vibrational frequencies than water molecules directly interacting with the interfacial sulfonate head groups. For complete spectral diffusion to occur, all water molecules must sample all frequencies, which means that they must experience all structures. A water molecule surrounded by other water molecules will have to diffuse to the interface before spectral diffusion can be completed. Diffusion to the interface, or perhaps exchange between populations, will be very slow in the extremely crowded and constrained environment of a very small reverse micelle water nanopool.

What might give rise to the 10 ps intermediate component that is not present in bulk water? The key difference between bulk water and water in the small reverse micelle is the strong influence of the interface on all of the water molecules. Water hydroxyls are either directly interacting with the interface or bound to a water that is directly interacting with the interface. Even though on average AOT reverse micelles are spherical, the interface is far from a smooth sphere. The interface has a rough topography, and studies have shown the necessity of including surface roughness in MD simulations in order to capture accurate lineshapes.[35] Water at the rough interface is shown schematically in the cartoon in Fig. 9. This rough topography will contribute to inhomogeneous broadening, as the water molecules must accommodate this topography. The hydrogen bonding network will be forced out of the ideal structure it can assume in bulk water. Individual sulfonate head groups can move relatively rapidly. Such motions will change the local hydroxyl environment and produce some spectral diffusion. Then one possibility is that fluctuations in the interfacial topography could be responsible for the 10 ps component of the spectral diffusion. According to our beat subtraction study, it does not appear that the identity of

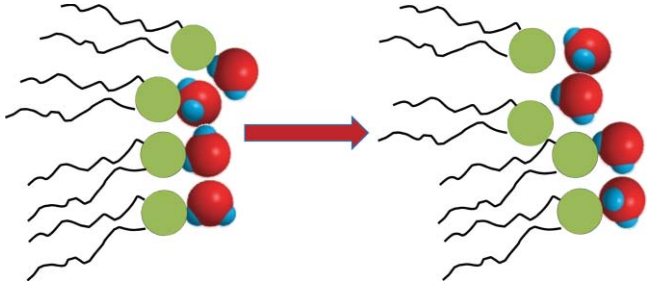

FIG. 9. Cartoon illustrating how topography changes through movements of individual sulfonate head groups in the surfactant shell of the reverse micelle can change the environments felt by the water molecules.

the solvent would affect the degree of surface roughness or fluctuations, given that the time constants remain the same for both systems.

Returning to Table IV, the FFCF has a homogeneous (motionally narrowed) component. The homogeneous component can be quantified by the dephasing time, T_2. The time constant t_1 has been attributed to fluctuations in the hydrogen bond network, and t_2 describes possible topography fluctuations or other dynamics induced by the presence of the interface. Each time constant has an associated frequency amplitude (Δ_i) which describes how much each component contributes to the linewidth. The intermediate component (t_2) adds a significant amount of inhomogeneous broadening, more than Δ_1. The parameter Δ_3 corresponds to the component described by an offset in the biexponential fit and reflects very slow dynamics outside of the experimental time window. This component is also large.

IV. CONCLUDING REMARKS

Here we have compared four experimental observables of the nature of the water nanopool in small AOT reverse micelles in two solvents: isooctane and CCl_4. The OD stretch of dilute HOD was studied. It was found that the linear absorption spectra were identical for reverse micelles in the two solvents. Polarization and wavelength selective pump–probe experiments showed that the vibrational lifetimes and orientational relaxation were independent of the solvent. Both of these time-dependent observables are quite sensitive to the local environment of the HOD. Ultrafast 2D IR vibrational echo spectroscopy, which measures spectral diffusion, provides detailed information on structural dynamics of the water hydrogen bonded network that is not accessible to other techniques. The initial studies of the AOT reverse micelles with isooctane as the solvent produced results that were inconsistent with expectation based on a large number of previous experiments on aqueous systems.[38,41,74,75] In particular, the individual interferograms had features that were inconsistent with water signals (see Figs. 7 and 8). Although isooctane is often used to form AOT reverse micelles, the problems with the interferograms led to performing the 2D IR vibrational echo measurements with CCl_4 as the solvent. The experiments with CCl_4 did not have the problematic interferograms observed with the isooctane solvent. The efficacy of using CCl_4 led to the necessity of demonstrating that the choice of solvent did not significantly change the properties of the water nanopools. As shown above, the nature of the water in the reverse micelles nanopools is independent of whether CCl_4 or isooctane is used as the solvent.

Examination of the AOT/isooctane system without the HOD in the water and without any water at all showed that the combination of AOT and isooctane gave rise to a signal with beats that do not occur under the same conditions with AOT/CCl_4. The beat pattern observed in the interferograms of the AOT/isooctane system (see Figs. 7 and 8) prompted the development of a 2D background subtraction procedure which was relatively successful in removing the solvent background from the true vibrational echo signal from the OD stretch. The observation of the solvent contribution to the desired signal is an important warning to other workers using 2D IR spectroscopy. It is generally assumed that the solvent will not give a well defined signal that can influence the signal from a resonant vibrational chromophore. Clearly this is not always the case. 2D background subtraction may be useful in other systems that give rise to a solvent contribution to the 2D spectra.

It is interesting to note that neither of the AOT stock solutions in isooctane and CCl_4 produce a background signal, nor does isooctane by itself. We also found that AOT/cyclohexane does not produce a signal. It was observed in a different type of 2D experiment that AOT/octane did produce a background signal, but that it is smaller than that with AOT/isooctane.[73] Therefore, the methyl groups are implicated as interacting with AOT in some manner to permit the background signal to occur.

The 2D IR vibrational echo experiments on the water nanopools of $w_0 = 2$ AOT/CCl_4 reverse micelles displayed dynamics on several time scales. In addition to a substantial motionally narrowed homogeneous component, relatively fast fluctuations on an $\sim$1 ps time scale contribute to spectral diffusion. These fluctuations are likely due to very local length fluctuations of hydrogen bonds. This time scale is somewhat longer than that found in bulk water for the same process. An intermediate time scale ($\sim$10 ps) does not have an analog in bulk water. This component probably arises from the influence of the interface on hydrogen bond dynamics. There are longer time scale fluctuations that are outside of the experimental time window, such as diffusion and exchange, which are limited by the vibrational lifetime of the OD hydroxyl stretch. The vibrational echo studies are currently being extended to larger reverse micelles ($w_0 = 4$, 7.5, 12, and 16.5).

ACKNOWLEDGMENTS

This work was supported by the Department of Energy (DE-FG03-84ER13251), the National Institutes of Health (NIH) (2-R01-GM061137-09), and the National Science Foundation (NSF) (DMR 0652232). Both E.E.F. and D.B.W. thank Stanford for Graduate Research Fellowships.

[1] D. Laage and J. T. Hynes, Science **311**, 832 (2006).
[2] D. Laage and J. T. Hynes, J. Phys. Chem. B **112**(45), 14230 (2008).
[3] D. E. Moilanen, E. E. Fenn, D. Wong, and M. D. Fayer, J. Phys. Chem. B **113**, 8560 (2009).

[4]D. E. Moilanen, E. E. Fenn, D. Wong, and M. D. Fayer, J. Am. Chem. Soc. **131**, 8318 (2009).
[5]D. E. Moilanen, E. E. Fenn, D. Wong, and M. D. Fayer, J. Chem. Phys. **131**, 014704 (2009).
[6]A. Tokmakoff, J. Chem. Phys. **105**(1), 1 (1996).
[7]V. M. Kenkre, A. Tokmakoff, and M. D. Fayer, J. Chem. Phys. **101**, 10618 (1994).
[8]K. A. Merchant, D. E. Thompson, and M. D. Fayer, Phys. Rev. Lett. **86**(17), 3899 (2001).
[9]M. Zulauf and H.-F. Eicke, J. Phys. Chem. **83**, 480 (1979).
[10]T. Kinugasa, A. Kondo, S. Nishimura, Y. Miyauchi, Y. Nishii, K. Watanabe, and H. Takeuchi, Colloids Surf., A **204**(1–3), 193 (2002).
[11]H.-F. Eicke and J. Rehak, Helv. Chim. Acta **59**(8), 2883 (1976).
[12]I. Piletic, D. E. Moilanen, D. B. Spry, N. E. Levinger, and M. D. Fayer, J. Phys. Chem. A **110**, 4985 (2006).
[13]C. Izquierdo, M. L. Moya, J. L. Usero, and J. Casado, Monatsch. Chem. **123**, 383 (1992).
[14]H. S. Tan, I. R. Piletic, R. E. Riter, N. E. Levinger, and M. D. Fayer, Phys. Rev. Lett. **94**(5), 057405 (2005).
[15]D. Cringus, A. Bakulin, J. Lindner, P. Vohringer, M. S. Pshenichnikov, and D. A. Wiersma, J. Phys. Chem. B **111**(51), 14193 (2007).
[16]D. Cringus, J. Lindner, M. T. W. Milder, M. S. Pshenichnikov, P. Vohringer, and D. A. Wiersma, Chem. Phys. Lett. **408**, 162 (2005).
[17]A. M. Dokter, S. Woutersen, and H. J. Bakker, Phys. Rev. Lett. **94**, 178301 (2005).
[18]A. M. Dokter, S. Woutersen, and H. J. Bakker, Proc. Natl. Acad. Sci. U.S.A. **103**, 15355 (2006).
[19]H.-S. Tan, I. R. Piletic, and M. D. Fayer, J. Chem. Phys. **122**, 174501 (2005).
[20]I. R. Piletic, H. S. Tan, and M. D. Fayer, J. Phys. Chem. B **109**(45), 21273 (2005).
[21]I. Piletic, H.-S. Tan, D. E. Moilanen, D. B. Spry, and M. D. Fayer, in *Femtochemistry VII: Fundamental Ultrafast Processes in Chemistry, Physics, and Biology*, edited by A. W. Castleman and M. L. Kimble (Elsevier, Amsterdam, 2006), pp. 195.
[22]D. E. Moilanen, N. Levinger, D. B. Spry, and M. D. Fayer, J. Am. Chem. Soc. **129**(46), 14311 (2007).
[23]P. Grigolini and M. Maestro, Chem. Phys. Lett. **123**(3), 248 (1986).
[24]P.-O. Quist and B. Halle, J. Chem. Soc., Faraday Trans. 1 **84**(4), 1033 (1988).
[25]D. Pant, R. E. Riter, and N. E. Levinger, J. Chem. Phys. **109**, 9995 (1998).
[26]R. E. Riter, D. M. Willard, and N. E. Levinger, J. Phys. Chem. B **102**(15), 2705 (1998).
[27]A. Douhal, G. Angulo, M. Gil, J. A. Organero, M. Sanz, and L. Tormo, J. Phys. Chem. B **111**(19), 5487 (2007).
[28]M. Ueda and Z. A. Schelly, Langmuir **5**(4), 1005 (1989).
[29]P. E. Zinsli, J. Phys. Chem. **83**(25), 3223 (1979).
[30]K. Bhattacharyya, Acc. Chem. Res. **36**(2), 95 (2003).
[31]M. R. Harpham, B. M. Ladanyi, N. E. Levinger, and K. W. Herwig, J. Chem. Phys. **121**, 7855 (2004).
[32]N. Nandi, K. Bhattacharyya, and B. Bagchi, Chem. Rev. **100**(6), 2013 (2000).
[33]S. Abel, F. Sterpone, S. Bandyopadhyay, and M. Marchi, J. Phys. Chem. B **108**(50), 19458 (2004).
[34]J. Faeder and B. M. Ladanyi, J. Phys. Chem. B **104**(5), 1033 (2000).
[35]P. A. Pieniazek, Y.-S. Lin, J. Chowdhary, B. M. Ladanyi, and J. L. Skinner, J. Phys. Chem. B **113**, 15017 (2009).
[36]S. Woutersen, U. Emmerichs, and H. J. Bakker, Science **278**, 658 (1997).
[37]T. Steinel, J. B. Asbury, and M. D. Fayer, J. Phys. Chem. A **108**, 10957 (2004).
[38]J. B. Asbury, T. Steinel, K. Kwak, S. A. Corcelli, C. P. Lawrence, J. L. Skinner, and M. D. Fayer, J. Chem. Phys. **121**, 12431 (2004).
[39]J. J. Loparo, S. T. Roberts, and A. Tokmakoff, J. Chem. Phys. **125**, 194521 (2006).
[40]J. J. Loparo, S. T. Roberts, and A. Tokmakoff, J. Chem. Phys. **125**, 194522 (2006).
[41]J. B. Asbury, T. Steinel, C. Stromberg, S. A. Corcelli, C. P. Lawrence, J. L. Skinner, and M. D. Fayer, J. Phys.Chem. A **108**, 1107 (2004).
[42]J. Stenger, D. Madsen, J. Dreyer, P. Hamm, E. T. J. Nibbering, and T. Elsaesser, Chem. Phys. Lett. **354**(3), 256 (2002).
[43]J. Stenger, D. Madsen, P. Hamm, E. T. J. Nibbering, and T. Elsaesser, J. Phys. Chem. A **106**(10), 2341 (2002).
[44]C. J. Fecko, J. D. Eaves, J. J. Loparo, A. Tokmakoff, and P. L. Geissler, Science **301**(5640), 1698 (2003).
[45]C. J. Fecko, J. J. Loparo, S. T. Roberts, and A. Tokmakoff, J. Chem. Phys. **122**, 054506 (2005).
[46]R. Rey, K. B. Moller, and J. T. Hynes, J. Phys. Chem. A **106**, 11993 (2002).
[47]C. P. Lawrence and J. L. Skinner, J. Chem. Phys. **117**, 8847 (2002).
[48]A. Piryatinski and J. L. Skinner, J. Phys. Chem. B **106**, 8055 (2002).
[49]A. Piryatinski, C. P. Lawrence, and J. L. Skinner, J. Chem. Phys. **118**(21), 9672 (2003).
[50]C. P. Lawrence and J. L. Skinner, Chem. Phys. Lett. **369**, 472 (2003).
[51]C. P. Lawrence and J. L. Skinner, J. Chem. Phys. **118**, 264 (2003).
[52]S. Corcelli, C. P. Lawrence, and J. L. Skinner, J. Chem. Phys. **120**, 8107 (2004).
[53]S. A. Corcelli, C. P. Lawrence, J. B. Asbury, T. Steinel, M. D. Fayer, and J. L. Skinner, J. Chem. Phys. **121**(18), 8897 (2004).
[54]R. Rey, K. B. Moller, and J. T. Hynes, Chem. Rev. **104**(4), 1915 (2004).
[55]K. B. Møller, R. Rey, and J. T. Hynes, J. Phys. Chem. A **108**, 1275 (2004).
[56]K. J. Gaffney, I. R. Piletic, and M. D. Fayer, J. Chem. Phys. **118**, 2270 (2003).
[57]S. Woutersen and H. J. Bakker, Nature (London) **402**(6761), 507 (1999).
[58]Y. L. A. Rezus and H. J. Bakker, J. Chem. Phys. **123**, 114502 (2005).
[59]D. E. Moilanen, E. E. Fenn, Y. S. Lin, J. L. Skinner, B. Bagchi, and M. D. Fayer, Proc. Natl. Acad. Sci. U.S.A. **105**(14), 5295 (2008).
[60]P. L. Luisi, M. Giomini, M. P. Pileni, and B. H. Robinson, Biochim. Biophys. Acta **947**(1), 209 (1988).
[61]D. Gómez-Diaz, J. C. Mejuto, and J. M. Navaza, J. Chem. Eng. Data **51**, 409 (2006).
[62]R. Trebino, K. W. DeLong, D. N. Fittinghoff, J. N. Sweetser, M. A. Krumbugel, B. A. Richman, and D. J. Kane, Rev. Sci. Instrum. **69**, 3277 (1997).
[63]K. Kwak, D. E. Rosenfeld, and M. D. Fayer, J. Chem. Phys. **128**(20), 204505 (2008).
[64]S. Park, K. Kwak, and M. D. Fayer, Laser Phys. Lett. **4**, 704 (2007).
[65]K. Kwak, S. Park, I. J. Finkelstein, and M. D. Fayer, J. Chem. Phys. **127**, 124503 (2007).
[66]S. Mukamel, *Principles of Nonlinear Optical Spectroscopy* (Oxford University Press, New York, 1995).
[67]J. R. Schmidt, S. A. Corcelli, and J. L. Skinner, J. Chem. Phys. **123**, 044513 (2005).
[68]J. R. Schmidt, S. T. Roberts, J. J. Loparo, A. Tokmakoff, M. D. Fayer, and J. L. Skinner, Chem. Phys. **341**, 143 (2007).
[69]G. Lipari and A. Szabo, J. Am. Chem. Soc. **104**(17), 4546 (1982).
[70]S. A. Egorov and B. J. Berne, J. Chem. Phys. **107**, 6050 (1997).
[71]E. E. Fenn, D. E. Moilanen, N. E. Levinger, and M. D. Fayer, J. Am. Chem. Soc. **131**, 5530 (2009).
[72]M. Freda, G. Onori, A. Paciaroni, and A. Santucci, Chem. Phys. Lett. **348**, 311 (2001).
[73]J. C. Wright, personal communication (August 1, 2010).
[74]S. Park and M. D. Fayer, Proc. Natl. Acad. Sci. U.S.A. **104**(43), 16731 (2007).
[75]D. E. Moilanen, D. Wong, D. E. Rosenfeld, E. E. Fenn, and M. D. Fayer, Proc. Natl. Acad. Sci. U.S.A. **106**(2), 375 (2009).
[76]See supplementary material at http://dx.doi.org/10.1063/1.3532542 for FT-IR spectra of the solvents and stock solutions, as well as additional information concerning the echo beat patterns.